Enkhzul et al., 2022. Mongolian Geoscientist 27 (54)
DOI: https://doi.org/10.5564/mgs.v27i54.1810

Mongolian Geoscientist

Original Article

Investigation of the electrical resistivity structure of the subsurface at Mogod valley in central Mongolia: Insight is using 1D Magnetotelluric inversion

Bayartogtokh Enkhzul[1*], Erdenechimeg Batmagnai[2], Shoovdor Tserendug[1], Gendenpuntsag Bayanjargal[1]

[1]*Department of Geomagnetism, Institute of Astronomy and Geophysics, Mongolian Academy of Sciences, Ulaanbaatar 13343, Mongolia*
[2]*Department of Earth Science, Institute of Geophysics, ETH Zurich, 8092 Zurich, Switzerland*

**Corresponding author: enkhzul@iag.ac.mn, ORCID: 0000-0001-9371-2960*

ARTICLE INFO

***Article history*:**
Received 09 March, 2022
Revised 28 June, 2022
Accepted 10 July, 2022

ABSTRACT

In this paper, we report a preliminary result of the Magnetotelluric investigation of the Mogod area. The Mogod region is one of the most prominent fields for geophysical study since the region includes young and active faults and geothermal activities. We conducted magnetotelluric measurements at 20 sites during geophysical field seasons in 2018-2021 as a pilot survey to understand data property and the electromagnetic noise level for the detailed electromagnetic studies. During the fieldwork, we used Lemi Magnetotelluric instruments and measured all three orthogonal components of the magnetic field and the horizontal components of the electric field. For the data processing, we used Matlab code by using the M-estimate regression method, and estimated the magnetotelluric transfer function with a low-noise level. The electrical resistivity model of the subsurface of survey layout shows us the existing resistivity anomalies at shallow-depth, and thickness of the upper crust approximately 11-17 km. Here, suggest that the thickness of the upper crust is 17 km and crust is 40 km with local magnetotelluric measurements. Additionally, the electric conductor appears in the southwest of Mogod region, we interpret that conductor play as a source of geological activity of Mogod region, and it might be the signature of a remanent fluid.

Keywords: resistivity anomaly, geophysical modeling, data processing

INTRODUCTION

For a clear geoscientific explanation of Earth's structure, we need to determine the upper crustal structure since most of the geological activities are going and driven by geotectonic mechanisms in the upper crust. Geophysical methods are very useful for the imaging deep structure up to Earth's inner core from the surface, as well as the electrical resistivity could give us additional information for the geological interpretation (Simpson and Bahr, 2005) such as the deep-root of fault, the hydrothermal activity, a connection of the rocks, and composition of materials (Munoz, 2014). The Magnetotelluric MT method can be one of an option to use geophysical prospection or geoscientific explanation such as a study that purposed to understand the mystery of the upper crust mechanism. Because, firstly, MT can determine the electrical resistivity of the structure, secondly, the sounding depth is more than enough for the upper crustal deep (Simpson and Bahr, 2005).

The MT became a common method for deep EM study since many of the MT investigations are successful and the results could give important explanations for the geoscience. MT method is based on measuring the temporal variation of the natural electromagnetic EM field that carries information about the electrical resistivity or resistivity of the medium. In our case, the medium for investigation is the subsurface of the Earth. Since the middle of the 20^{th} century, the MT method has been developed (Rikitake, 1948; Tikhonov, 1950; Cagniard, 1953), and currently, the 3D electrical resistivity distribution is determined by strong computational tools and machines (Egbert and Booker, 2012). The novel MT study was implemented as a joint project in Mongolia from 2016 to 2018, which study carried out the latest explanation for the deep structure of central Mongolia including Khangai, Gobi-Altai mountain range by fully covering the MT measurements (Käufl et al., 2020). Although during this project, we learned more details of the MT method for measuring MT field and processing data, we had no chance to do MT study individually since had no owned equipment. Since 2019, we started to prepare more solid scientists for the MT investigation with an ongoing geothermal exploration project in the Mongolian Khangai dome (Batmagnai et al., 2019, 2020). With the geothermal project, we equipped Lemi-423 MT instruments to measure EM-fields variations, which produced in LVIV of Ukraine. MT equipment gives us the potential to conduct EM measurements and testing recently developed methods. Our latest studies are focused on the 1D, 2D MT modeling, we currently investigated more details of the 1D MT modeling by using the analytic solution of Helmholtz's equation to predict data from the synthetic model, which is so-called a direct solution or forwarding, and for the indirect solution or inversion which is purposed to find a the-best fitted model from observed data, we use gradient-based non-linear optimization techniques such as the quasi-Newton and Levenberg-Marquardt (Enkhzul and Batmagnai, 2021). For the 2D investigation, we solved the forward problem or 2D Maxwell's equation by using the finite-difference numerical approach (Enkhzul and Batmagnai, 2021a). One of the goals of this study is the use of novel developed techniques for newly collected MT data at the Mogod field. The Mogod study area is located in the eastern part of the Khangai dome.

The Khangai dome located in central Mongolia is an intra-continental mountain range stretching from the Siberian and the Indo-Asian tectonic plate margins. The Khangai region has been described as a dome (Windley and Allen, 1993; Cunningham, 2001). The basement of the Khangai dome consists Pre-Cambrian block that contains tonalitic and trondhjemitic gneisses, potassic granitoid and various migmatites, and high-grade schists and gneisses (Kepezhinskas, 1986). The Khangai region consists of intensely deformed Carboniferous-Devonian and not wide distributed Permian Triassic sedimentary rocks which were deposited on basement intruded by late Paleozoic and early Mesozoic granite and granodiorite huge bodies. Late Cenozoic numerous high potassium alkaline basaltic provinces are distributed throughout the Khangai area. They are covered by unconsolidated Quaternary sediments. The most Cenozoic volcanos are located in the eastern part of the Khangai dome where the hydro-geothermal system is one of the best in terms of quality of the fluid heat-carrier with a high yield of thermal source as it is the situation in an area of an ancient deep magma chamber and the lasting a high Cenozoic volcanic activity.

The Mogod sum, located 70 km southwest of Bulgan aimag, exposes intermediate-volcanic rocks of the Khanui Group and the Mogod Formation (Tsukada et al., 2008; Batbayar et al., 2014). Fig. 1 shows the geographical and geological formation of the study area. The Mogod Formation's volcanic rocks are composed of intermediate vesicular lava, tuff breccia, and conglomerate formed by a volcanic mudflow. The lava, fine- to coarse-grained, has porphyritic, aphyric, or trachytic textures with and hornblende. The lava has platy and columnar joints and partly includes abundant fragments of intermediate lava. The vesicles of

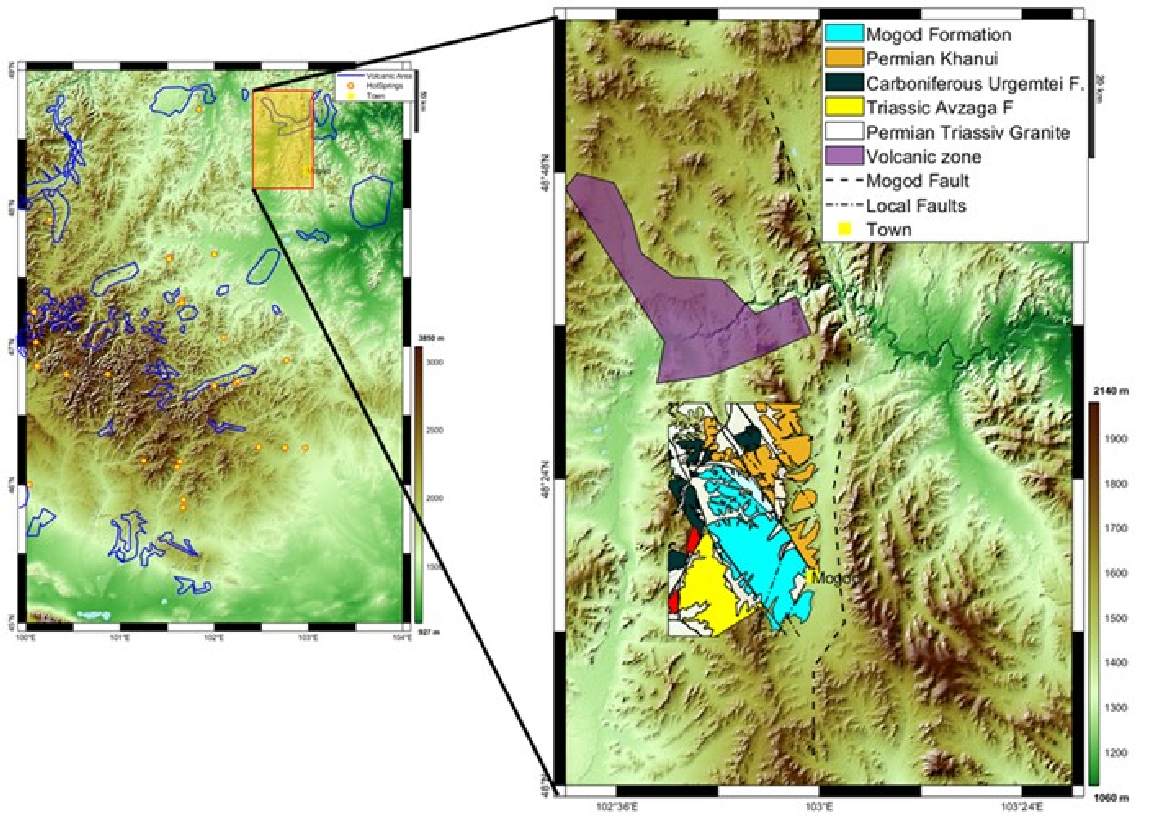

Fig. 1. A map of the topographic of the Khangai region in regional (left) and local scale of the study area with some information of formation (Tsukada et al., 2008) and volcanic basalts (Ancuta et al., 2018)

the lava, partly filled with calcite or chlorite, forms amygdule. The volcanic rocks of the Permian- Triassic igneous rocks can be divided into the Lower Permian Mogod Formation, the Lower-Upper Permian Khanui Group, and the Upper Permian Bugat/Baruunburen Formation. The K-Ar age of intermediate lava of Mogod formation is described that 292±14 Ma. One of the hot springs, which is the so-called Khulij exists in Mogod sum. Khulij hot springs are one of the good indicators for the existing deep-rooted geothermal activity in the Mogod region.

Additionally, the study area is one of the areas with high seismic activity, and according to the latest study (Baldulam and Odonbaatar, 2019) most of the earthquakes in this region occur along the Mogod and Bayan-Agt faults. During the 20^{th} century, >4 Mw events are registered before 1960. An earthquake with a magnitude of Mw 7 is occurred at the Tulee-Uul in Mogod sum on 5 January 1967, when the long fault created. From 1900 until 2017, ~22000 earthquake events with a magnitude of 0.1-7.1 Mw are recorded in the historical note and seismometer in the Mogod region. Hence Mogod region, which became one of the strongest seismic active zones on the dense population centers such as Mogod sum, Bulgan aimag as well as capital city Ulaanbaatar.

In this study, we report a preliminary result of the MT investigation at the Mogod region. The advantage of this study is we obtained the first results that subsurface structure up to the bottom of the upper crust, which results give us the potential for the next detailed investigations such as correlations between seismicity and deep conductor or the geothermal exploration.

MT METHOD

MT method is geophysical a passive-sounding method that is one of the electromagnetic techniques to probe the electrical resistivity of the subsurface of the Earth. During the MT survey, we measure the Earth's electromagnetic responses, which is the so-called transfer function. The MT transfer functions are functionally related to the frequency of EM signals and site location (Egbert and Booker, 1986).

One of the MT transfer functions is the impedance tensor $\boldsymbol{Z}$, which is the relation between the horizontal electric and magnetic components in the frequency domain. The impedance tensor $\boldsymbol{Z}$ is a second rank tensor, which contains complex-valued scalar impedances (eq.1).

$$Z(r,\omega) = \begin{pmatrix} Z_{xx} & Z_{xy} \\ Z_{yx} & Z_{yy} \end{pmatrix} \quad (1)$$

The impedance tensor gives us information about the 1D, 2D and 3D electrical resistivity distribution of the subsurface (Bredechivsky and Dmitriev, 2008; Simpson and Bahr, 2005). From the impedance tensors, we compute the physical parameters such as the apparent resistivity and the impedances phases (eq.2).

$$\rho_a = \frac{|Z_{ij}|^2}{\omega\mu}, \quad \phi = atan^{-1}\left(\frac{Im(Z_{ij})}{Re(Z_{ij})}\right), \quad ij = xy \quad (2)$$

The apparent resistivity is measured weighted average of true resistivities of the subsurface at the surface.

SSQ impedance

Galvanic distortion, which is related near-surface lateral heterogeneities, makes a challenge for the MT modelling of impedance tensors. In this case, one of the solutions to avoid distortion effects is the using the regional electrical resistivity model as a starting model for the inverting the impedance tensors in 3D scenario. Berdichevsky et al., (1980) showed that the regional impedance can be obtained by geometric average of the determinant of impedance tensors, and suggested that distortion coefficient. Sum of squared elements of the impedance tensor or so-callled SSQ impedance, which is introduced by Rung-Arunwan et al., (2016) is reexamined version Berdichevsky average. SSQ impedance, $\boldsymbol{Z_{ssq}}$ (Eq, 5) is well indicator of the local and regional distortion as well as site gain, which is related with the static-shift effects (1989, 2016).

$$Z_{ssq} = \sqrt{\frac{Z_{xx}^2 + Z_{xy}^2 + Z_{yx}^2 + Z_{yy}^2}{2}} \quad (3)$$

1D inversion

The main goal of the MT inversion problem is to find the unknown electrical resistivity (***m***-model**)** structure of the subsurface of the Earth from observed impedance tensor $\boldsymbol{d_{obs}}$. The predicted $\boldsymbol{d_{pre}}$ is obtained by the direct solution of Maxwell's equations in the frequency domain. We consider the relationship between the predicted data ($\boldsymbol{d_{pre}}$) and model ($\boldsymbol{m}$) in the following form

$$d_{pre} = F(m) \quad (4)$$

$$m = F^{-1}d \quad (5)$$

where $\boldsymbol{F}$ is the matrix $\boldsymbol{n \times n}$ which is so-called the forward operator and contained the solution of Maxwell's equation in 1D, 2D, 3D medium. In the 1D case, we consider Wait's recursion formula (Wait, 1953) which is the solution of Maxwell's equation for the 1D horizontally layered half-space.

To find unknown model |($\boldsymbol{m}$) we consider the indirect solution of eq.3, (eq.4). This is an inversion procedure of MT modeling. With inversion, we can predict the best-fitted model (m) from the observed data ($\boldsymbol{d_{obs}}$.). Usually, the geophysical inversion problem is characterized as a non-linear and ill-posed problem. Therefore, we use unconstrained optimization methods such as gradient and probabilistic algorithms. In this study, we use a recently developed 1D inversion code (Batmagnai et al., 2020; Enkhzul and Batmagnai, 2021b) which is implemented on the Matlab programming language with the multi-selections of the deterministic algorithms.

MT data

MT data were collected at 10 sites in the Mogod field in autumn of 2020. The main point of this survey was understanding about EM noise level of the Mogod village. Enkhzul and Batmagnai (2021b), conclude that MT data are affected by cultural noises such as electric power lines and their utilization, and using remote reference can be the best option to reduce noise from the signals. With this approach, we used the 0100B site for the estimating transfer function as a remote reference site (Fig. 2, blue square). In 2021, during the fieldwork, we collected 10 MT sites along the line with a length of >100 km.

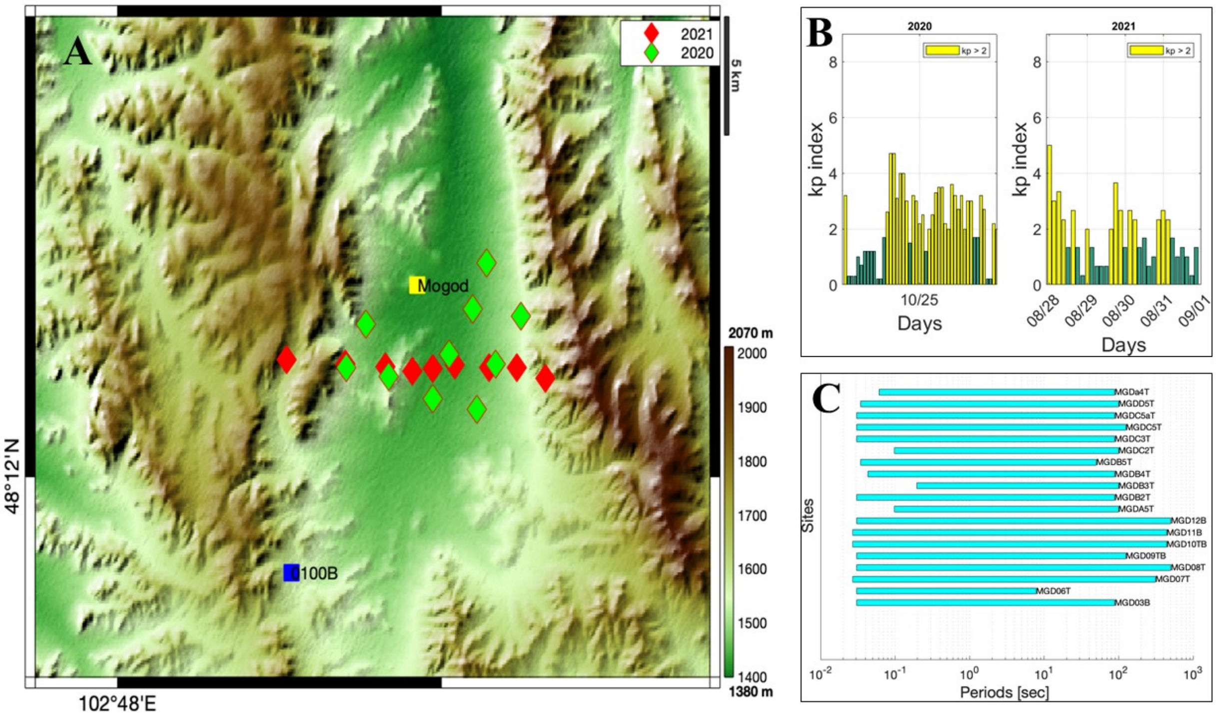

Fig. 2. MT sites, geomagnetic activity during the measurement and observed periods

The resulting is recovered a preliminary 2D electrical resistivity distribution Enkhzul and Batmagnai, (2021a) reported that a shallow depth conductor exists southwest of Mogod sum, by using those MT data.

Here, we more concentrated to create a comprehensive electrical resistivity model derived by 1D inversion. The first way to obtain the model was re-processing of the raw time-series with the remote reference site, and selection of time-window using a modified version of the processing code for LEMI-423 (Enkhzul and Batmagnai, 2021c). According to the source-field activity was high during field days in 2020 (Fig. 2, right-top), most of the stations are measured EM-field in 2 hours to 12 hours, but in 2021, we measured EM-field more than one day mostly. The main parameter of a source-field activation is ***kp*** index, which indicates the global geomagnetic storms with high values. During our fieldwork, ***kp*** index was not constantly low, it had a changed number of 1–5. Therefore, we recorded enough MT data associated with the interesting depth of this study. Here, we can consider that the quality of the MT responses is much better than previous studies (Enkhzul and Batmagnai, 2021c) based on the comparison with previous results from data processing (Fig. 3). We estimated the $\boldsymbol{Z_{ssq}}$ (eq.5) impedance supposed to obtain a regional resistivity. In Fig. 3 (left), we plotted a cloud of apparent resistivity and impedance phases of SSQ impedances of each MT site. in order to understand apparent resistivity shifts via galvanic distortion effects. The resulting is the amplitude of apparent resistivity of the survey area is varying from ~10^2 to ~10^4.

The dominated periods of MT signal at every site are recorded in periods of 0.02s to 100s (Appendix A), the shortest period (or the highest frequency) is 0.01s and the longest period (or the shortest frequency) is 1000s (Fig. 2C).

According to the C-responses, which gives us information about the depth of the center of mass of induced current at measured periods, the maximum depth of MT for this study is considered 70 km.

$$c = \sqrt{\frac{1}{i\omega\mu_0\sigma}} \qquad (6)$$

C-responses allows that the depth sensitivity of the observed impedance is 500 m 150 km. This study illustrates a 1D model surface to more

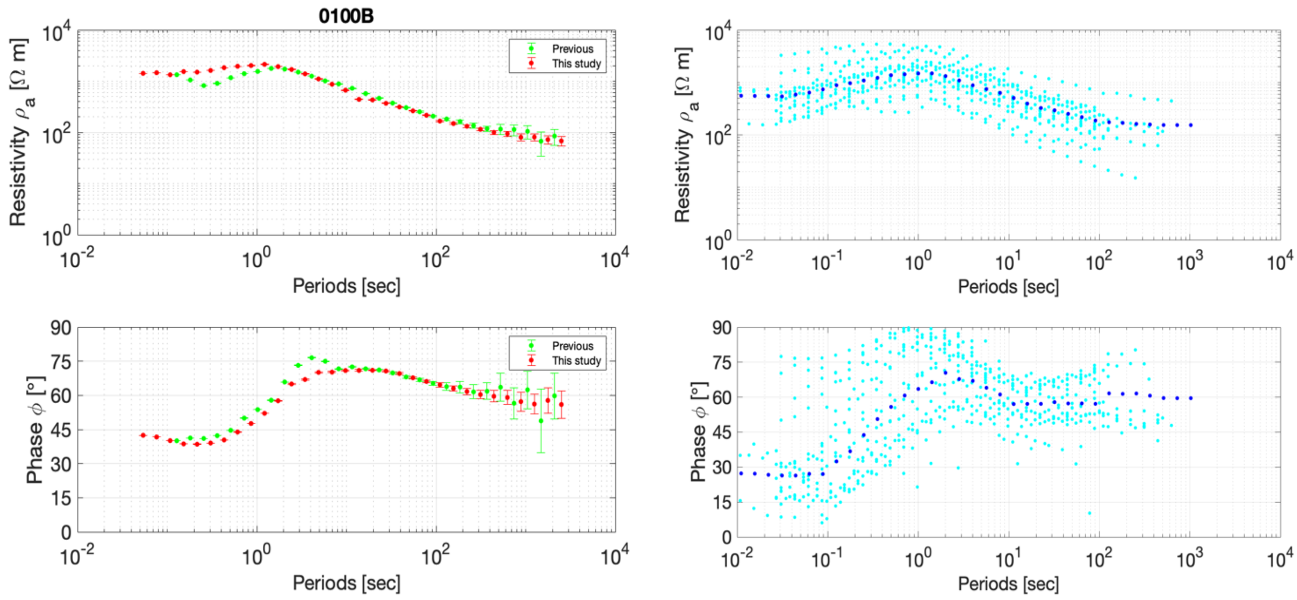

Fig. 3. MT responses show an improvement of the data quality (left), where red responses were evaluated by a new processing code and used for this study. And $\boldsymbol{Z_{ssq}}$ responses were estimated at every site and plotted in the right panel

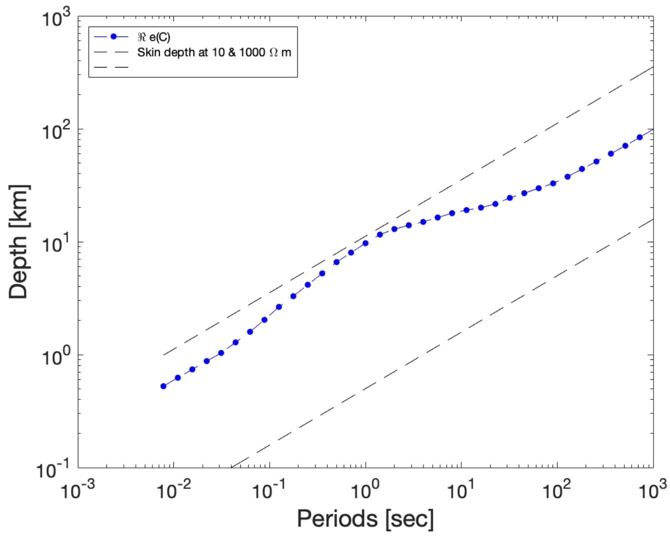

Fig. 4. The real part of C-response (blue dotted-curve, skin depths are calculated at 10 and 1000 Ωm homogeneous medium (black dashed lines)

than 150 km since it is characterized by an initial model selected by our assumption (described in the next section).

As we discussed above that data is affected by galvanic distortion in Fig 3, we used SSQ impedance supposed to strong effect of the static shift for the modelling. Appendix A shows the measured impedance tensor of MT site which are measured at Mogod valley.

The 1D electrical resistivity model

Generally, our inversion code is based on the gradient methods, so we need to take care of the priority of starting models. Therefore, we conducted the experimental steps in order to choose an initial model with a good model parameter. Here, we considered two different procedures to choose the initial model were selected from the testing. The first procedure is the user-based selection, where the user had only decided to give physical parameters for the initial model. During this experiment, we observed that the model updating was very sensitive and changeable related to the resistivity value of a homogeneous half-space initial model. Hence, we considered that using an average of observed apparent resistivity for the initial model setup is more efficient because gradient-based optimizations are more complicated to reach a global minimum with the random parameters (see, Enkhzul and Batmagnai, 2021b).

Although we could solve a complication of the starting resistivity of the initial model, we had an issue since the number of layers and their thicknesses have been manually selected until we obtain the best model. This issue became fundaments of the second procedure. The second procedure, so-called fully data-based initial model selection is based on the skin-depth effect of EM induction theory to estimate the thickness of the layers.

In the EM sounding, the skin depth or penetration depth is a major parameter to express an amplitude of EM wave at the specific depth (In theory, the EM signal is attenuated from the air-ground interface). Therefore, the skin depth is formulated as

$$\delta = 503\sqrt{\rho_a T} \tag{7}$$

The thicknesses of the layers of the initial model were estimated automatically by using the minimum penetration depth via the shortest period. Here, the following formula shows us that thickness of layers is increased power of 1.2, which is related to the period.

$$D = \delta_{min} \cdot 1.2^{[0:N]} \tag{8}$$

Where $\boldsymbol{\delta_{min}}$ is the minimum depth of penetration depth, and $\boldsymbol{N}$ is the length of observed periods.

Considering test runs of the inversion procedure, the approach which we mentioned above is verified that increases model resolution and decreases numerical errors.

The results of the $\boldsymbol{Z_{ssq}}$ tests are shown in Table.1, where we show the misfit of observed and predicted data from the different model parameters and the scaling factors.

According to the results in Table 1, we could see that the data-based resistivity and number of layers approach is a good option to use for selecting the initial model setup for the 1D inversion. Here, the scaling factor is only to the handling the smoothing of models.

The 1D inversion results of the $\boldsymbol{Z_{ssq}}$ impedance are represented in Fig 5, where the obtained models of several tests with the scaling factor 0.8 and their responses are plotted (Table 1 shaded by yellow). The initial model was parameterized by 35 layers with 550 Ωm half-space to obtain the best-fitted model. Here, we believe that the model (Fig. 5, red curves) can interpret the geoelectric characteristic of the subsurface moreover structure of the Earth layers since the observed data is explained by the 1D MT model. Finally, the misfit of observed and predicted data was reached 1.6 from 32 after 146 iterations. Overall, the model consists of whole-crust and top of upper mantle

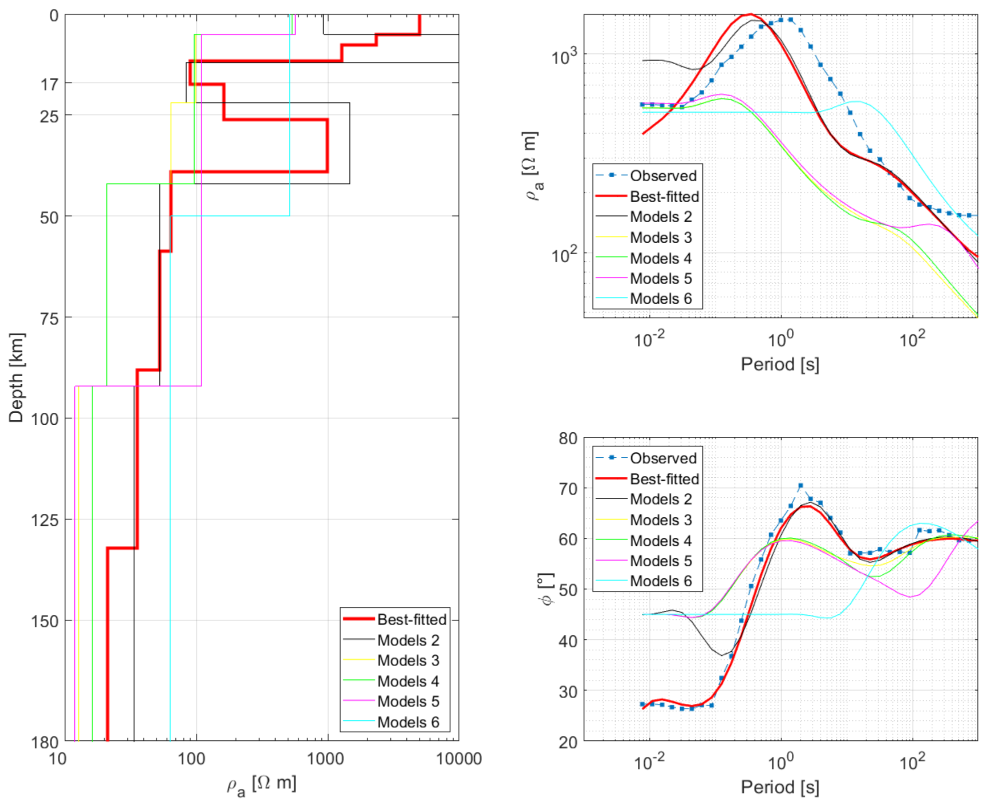

Fig. 5. 1D MT model of the $\boldsymbol{Z_{ssq}}$ responses, more details of the model is described in the main text

Table 1. Results of tests to choose an initial model for the 1D inversion setup

№	Models	Layers	Data based (Ωm)			User selected (1000 Ωm)		
			reg_2.5	reg_0.8	reg_1	reg_2.5	reg_0.8	reg_1
1	model_multi	35	1.6857	1.6358	1.6453	1.7624	1.7367	1.7301
2	model_2	6	2.54854	2.46132	2.47309	2.54856	2.46134	2.47308
3	model_3	5	4.3451	4.346	4.346	4.3451	4.346	4.346
4	model_4	4	4.347	4.3477	4.3477	4.347	4.347	4.3477
5	model_5	3	4.1934	4.1948	4.1947	4.1934	4.1947	4.1946
6	model_6	2	3.3961	3.3956	3.3956	3.396	3.3956	3.3956

and it can express the major layers or boundaries. In the next section, we will discuss a preliminary interpretation of the resistivity structure and its anomalies with respect to geological activities such as active fault and hydrothermal activity. As we discussed, we inverted Z_{xy} components of the impedance tensors for every site supposed to imagine the electrical resistivity structure of the study area at the corresponding depth of conductors by the horizontal slices.

With our approach to finding the best model, the sounding depth was moderately due to the difference of observed periods on the individual measurement (Fig. 6). However, this model is useful to determine the electrical resistivity anomaly of the upper crust with a better resolution.

DISCUSSION

The electrical resistivity model is recovered at the Mogod region by using the 1D inversion algorithm at 20 sites. In theory, it was possible to create the resistivity model as 2D or 3D but the measurement had only supposed for the statistical understanding. Since MT sites were sparsely in the study region, the best option was to a create 1D model. According to the real part of C-responses, the sounding depth is moderately changed 14-130 km whereas the layer numbers for the model for the measurement sites were obtained by using observed periods. Fig. 6 shows relative numbers of sounding depth and layers for every site. Overall, inversions were performed well, and the recovered electrical resistivity model was able to explain the regional structure of this region. This is an advantage of the measuring MT field study field as one of the geophysical methods to explain structure that MT gives information about regional structures with a few observation sites. According to the main goal of this study, non-regularity of the observation site and not enough MT sites, we only have concentrated on the regional structure of the study region. To increase the resolution of the MT model, we need to the clear thinking of the next fieldwork and modeling. Although in this study, we report a huge progression of the recently developed MT method in Mongolia, more detailed investigations are necessary such as an additional grid or line measurements to extend field area with fully covered dense sites and 2D or 3D modeling (but it is computationally expensive).

The advantage of more MT measurements is

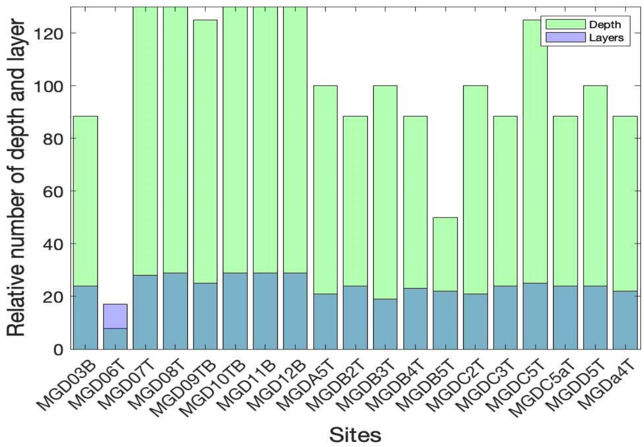

Fig. 6. The sounding depth range of layers and number of layers at every site, where the blue is the number of layers of the initial model in numbers, and green is maximum penetration depth in kilometer

very clear to say that we could understand the source or root of the geological activate of this region. Next paragraphs, we discuss more the interpretation of the 1D electrical resistivity model.

The major Earth layers such as the thickness of upper and lower crust, Moho depth, and sedimentary thickness are predicted from the 1D inversion result of the Z_{ssq} responses in this study. The surrounding of the geological structure of the Mogod area is usually explained by Precambrian blocks overlaid by Permian and Triassic rocks or sediments. According to recent studies, the effusive volcanic basalts due to flow lavas have existed corresponding to the ancient volcanic activity such as Uran Togoo and Ikh Togoo volcanos. With the electrical resistivity model, we could simplify the regional or coarse structure of the Earth layers.

From Fig. 7, we show the four main layers. The upper case of the first layer up to 5 km with the high resistivity of 5000 Ωm can be explained by the pre-Cambrian block, where we removed the effects from sedimentary resistivity anomalies at less than 3 km from the model. Then resistivity is decreased until 1000 Ωm at 11 km. From the 11 km, the resistivity decreases strongly with respect to the electric conductor, and at 17 km resistivity is increasing up 800 Ωm. Here, we suggest that the upper depth of the upper crust exists in this period range that 11-17 km. According to the study of geophysical study by (Zorin et al., 1990), we assume that the depth of boundary between upper and lower crust exists at 17 km. The strong conductor with a resistivity of >80 Ωm can be explained fluids. Because the study region is one of the locations which has geothermal activity.

The geoelectrical structure in 17-40 km is interpreted by the lower crust, where the electrical resistivity reaches <80 Ωm and the top of this layer could be explained by weak-crustal fluids since the other regional studies conclude that a weak crustal zone exists Khangai Dome (Käufl et al., 2020). With this study, we suggest that the local Moho depth beneath Mogod study region using our 1D model is 40 km. It can be a related study of (Zorin et al., 1990).

The top of upper mantle depths 40-75 km is

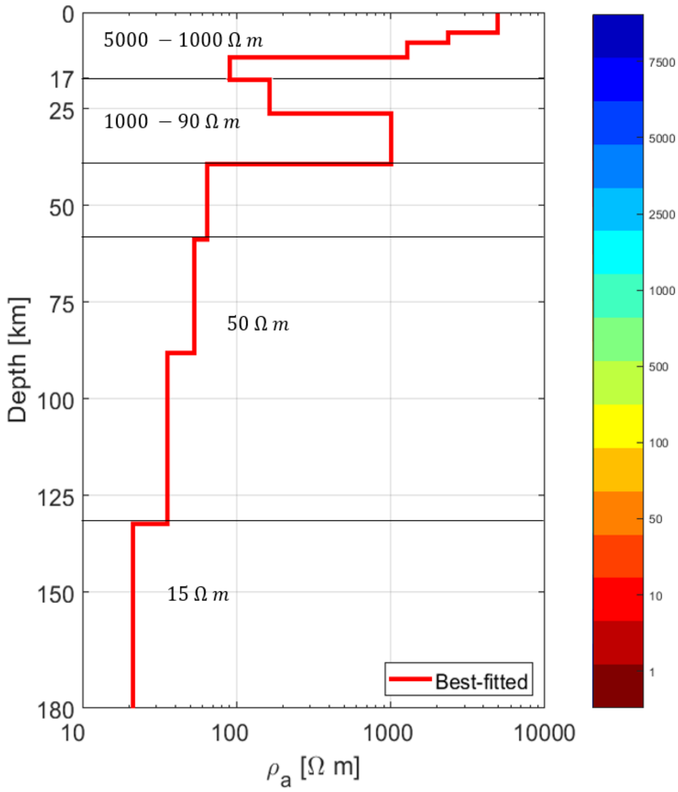

Fig. 7. 1D electrical resistivity model, which is obtained by geometric average of Z_{ssq} impedances

characterized by a moderate resistivity 800-90 Ω m. while depths below 125 km resistivity <50 Ω m and it can indicate the asthenosphere. Additionally, Bouguer gravity models revealed a localized low-density structure at a depth of 80-125 km below the central Khangai (Tiberi et al., 2008), coincident with the location of the low-resistivities of our model.

In previous studies (Käufl et al, 2020), the Khangai dome has been fully recovered by MT surveys but the previous study has attempted to understand the regional structure and how this relates to upwelling in the Khangai Dome. A huge distance separates the MT sites of the regional MT survey. There is no MT site within 50 km of Mogod. The novelty of this study to be the first to attempt an electrical resistivity model with local high resolution. However, the regional MT model helped to understand more deep resistivity structures.

The structure and lithology of Mogod Village expose intermediate volcanic rocks of the Khanui Group and the Mogod Formation. The

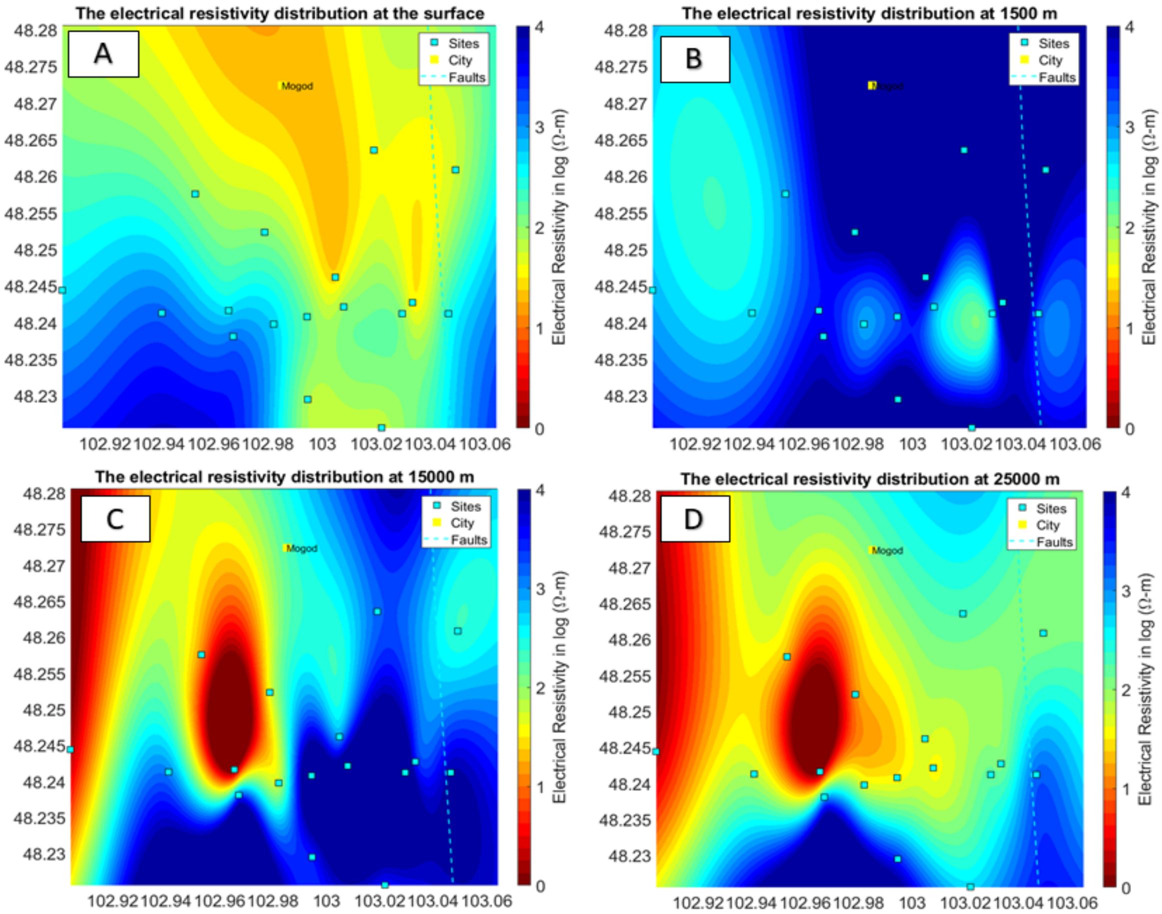

Fig. 8. Horizontal slices of the resistivity distributions at the surface, sea-level, 15000 m and 25000 m

Mogod Formation's volcanic rocks are composed of intermediate vesicular lava, tuff breccia, and conglomerate formed by a volcanic mudflow. Those formations are usually classified in the porous rocks therefore, the surface or near-surface structure of the Mogod valley must be low resistivity

We show surface structure in Fig. 8A. As we discussed the electrical resistivity is low and moderately at the first layer of the Earth, which can be related to pore sediments. But resistivity is increased by local 3D resistivity feature beneath Mogod valley (Fig. 8B), which can be related to the dry and massive basement rocks. It could be effective to more focus joint interpretation of local geology and MT data analysis in the next steps. However, we have very clear the electrical resistivity anomaly (Fig. 8C and D) exists in the upper crust beneath Mogod region. It can be explained by the accumulated fluid in the upper mantle. To clearly identify and clarify the conductor that is a signature of the ancient hydrothermal alteration, we need to more detail MT investigation and more petrophysical analysis. This is can be the reason for the next study's purpose to make a 3D grid measurement and invert them.

Geological activation at the study area is not clearly determined by our 1D based MT model, but we obtained some main ideas that can be related to the deep-root of the hydrothermal and earthquake activities. The deep conductor characterized at depth of 1500 m to lower crust can be corresponded with a remanent volcanic activity that can be a hot chamber consisting of a fluid or magmatic material, and geothermal fluid of Khulij hot springs heated by this structure. We observed a more interesting feature that has high resistivity beneath Mogod village. According to the geological map, it is more challenging to understand. However, we observed that an earthquake fault is crossed the contact zone between two different structures. It is not enough interpretation for the deep-root of the Mogod fault if the resistivity anomaly is only a bulk Precambrian block (Fig. 8B, C, and D). Therefore, we need a clear understanding of existing geophysical data and other geoscientific methods and obviously, more MT measurements are a preliminary purpose to make a very clear explanation of the deep-root.

Overall, this study carried out a general characteristic of the subsurface beneath Mogod region, we have missing information of the geological activities. Considering a huge resistive feature near-surface, we need to clear thinking with the geoscientific approaches. With integrated geophysical measurement and other information of geology and geochemistry, we need to find an answer for the several questions that can it possible the resistivity feature respect to the permafrost or gas otherwise dry hot rocks? The next studies will be more concentrated on finding answers to those scientific questions.

CONCLUSION

We report the results of a pilot MT survey at the Mogod region in this paper. Although MT measurements were supposed to investigate the MT noise level of this region, we studied a coarse deep electrical resistivity structure by using MT data since data quality was enough for the pilot study. This study carried out certain results for all of the chain to conduct MT studies such as the processing, modeling, and interpretations. According to those results, we conclude that 1) expecting MT survey in future must be done as soon as possible, and measurement will be conducted with the using low-pass filter and several days continue. 2) The using the techniques to decrease galvanic effects must be efficient to decrease the effect of the static shifts. 3) 1D modeling worked well and was good to use in future studies but in MT study areas such as Mogod, we need to make a 3D MT model and use a 1D model like a starting model, which could be decreased numerical errors for the inversion procedure. Overall, we tried to interpret MT results with the surface and background geology but we need a more clear understanding of geoscientific information to solve the challenges discussed in the last session.

ACKNOWLEDGEMENTS

Field survey was financially supported by the SNF, R4D, Switzerland and Mongolian Academy of Sciences. We thank the field team and our colleagues from Mongolian Academy of Sciences for their support to succeed fieldwork and collecting data. We also want to thank reviewers their detailed comments, which helped improve the paper.

REFERENCES

Ancuta, L.D., Zeitler, P.K., Idleman, B.D., Jordan, B.T. 2018. Whole-rock 40Ar/39Ar geochronology, geochemistry, and stratigraphy of intraplate Cenozoic volcanic rocks, central Mongolia. Bulletin, v. 130 p. 7-8, 1397-1408. https://doi.org/10.1130/B31788.1

Baldulam, Ch., Odonbaatar Ch. 2019. Seismic study of Bulgan aimag. Geophysics and Astronomy, v. 6, p. 5-11.

Batbayar, N., Takekawa, J.Y., Natsagdorj, T., Spragens, K.A., Xiao, X. 2014. Site selection and nest survival of the Bar-headed Goose (Anser indicus) on the Mongolian Plateau. Waterbirds, v. 37(4), p. 381-393. https://doi.org/10.1675/063.037.0405

Batmagnai, E., Tsegmed, B., Nasan-Ochir, T., Gantsogt, S., Eldew-Ochir, B. 2019. A pilot geomagnetic and magnetotelluric survey in Mogod area of the Eastern Khangai, Mongolia. Proceedings of the Mongolian Academy of Sciences, v. 59 (2), p. 71-81. https://doi.org/10.5564/pmas.v59i2.1220

Batmagnai, E., Samrock, F., Grayver, A., Kuvshinov, A. V., Saar, M.O., Demberel, S., Dolgorjaw, O. 2020. 3-D Magnetotelluric investigation of the mid-enthalpy geothermal region near Tsetserleg city in Mongolian Arkhangai province. In AGU Fall Meeting Abstracts, v. 2020, p. GP007-0011.

Berdichevsky, M.N., Dmitriev, V.I. 2008. Models and methods of magnetotellurics. Springer Science and Business Media, 564 p. https://doi.org/10.1007/978-3-540-77814-1

Berdichevsky, M.N., Vanyan, L.L., Kuznetsov, V.A., Levadny, V.T., Mandelbaum, M.M., Nechaeva, G.P., Shpak, I.P. 1980. Geoelectrical model of the Baikal region. Physics of the Earth and Planetary Interiors, v. 22(1), p. 1-11. https://doi.org/10.1016/0031-9201(80)90095-3

Cagniard, L. 1953. Basic theory of the magneto-telluric method of geophysical prospecting: Geophysics, v. 18(3), p .605-635.

Cunningham, W.D. 2001. Cenozoic normal faulting and regional doming in the southern Hangay region, Central Mongolia: implications for the origin of the Baikal rift province: Tectonophysics, v. 331(4), p. 389-411.

Egbert, G.D., Booker, J.R. 1986. Robust estimation of geomagnetic transfer functions. Geophysical Journal International: v. 87(1), p. 173-194. https://doi.org/10.1111/j.1365-246X.1986.tb04552.x

Enkhzul, B., Batmagnai, E. 2021a. 2-D Magnetotelluirc inversion and its application. Khureltogoot-2021, Ulaanbaatar, Mongolia, Nov, 2021.

Enkhzul, B., Batmagnai, E. 2021b. 1-D Magnetotelluric modelling derived by deterministic inversion methods. Geophysics and Astronomy, v. 8, p. 94-105.

Enkhzul, B., Batmagnai, E. 2021c. Data processing and modelling of Lemi-423 station. Geophysics and Astronomy, v. 8, p. 106-118.

Käufl, J.S., Grayver, A.V., Comeau, M.J., Kuvshinov, A.V., Becken, M., Kamm, J., Demberel, S. 2020. Magnetotelluric multiscale 3-D inversion reveals crustal and upper mantle structure beneath the Khangai and Gobi-Altai region in Mongolia. Geophysical Journal International, v. 221(2), p. 1002-1028. https://doi.org/10.1093/gji/ggaa039

Kepezhinskas, K.B. 1986. Structural-metamorphic evolution of late Proterozoic ophiolites and Precambrian basement in the Central Asian foldbelt of Mongolia. Precambrian research, v. 33(1-3), p. 209-223. https://doi.org/10.1016/0301-9268(86)90022-7

Munoz, G. 2014. Exploring for geothermal resources with electromagnetic methods. Surveys in geophysics, v. 35(1), p. 101-122. https://doi.org/10.1007/s10712-013-9236-0

Rikitake, T. 1948. Notes on electromagnetic induction within the Earth. Bulletin of the Earthquake Research Institute, v. 24(1), p.1-8.

Rung-Arunwan, T., Siripunvaraporn, W., Utada, H. 2016. On the Berdichevsky average. Physics of the Earth and Planetary Interiors, 253, 1-4. https://doi.org/10.1016/j.pepi.2016.01.006

Simpson, F., Bahr, K. 2005. Practical magnetotellurics. Cambridge University Press, 270 p. https://doi.org/10.1017/CBO9780511614095

Tiberi, C., Deschamps, A., Déverchère, J., Petit, C., Perrot, J., Appriou, D., Artemiev, A.A. 2008. Asthenospheric imprints on the lithosphere in Central Mongolia and Southern Siberia from a joint inversion of gravity and seismology (MOBAL experiment). Geophysical Journal International, v. 175(3), p. 1283-1297. https://doi.org/10.1111/j.1365-246X.2008.03947.x

Tikhonov, A.N. 1950. On determining electrical characteristics of the deep layers of the Earth's crust. In Doklady, v. 73(2), p. 295-297.

Tsukada, K., Umeda, K., Nadmid, B., Sodnom, K., Nuramkhaan, M. 2008. Ages from the "Mogod Formation" of the Permian-Triassic igneous rocks in the Sayan-Baikal belt, northern Mongolia. Bulletin of the Nagoya University Museum, v. 37, p 1-12.

Wait, J.R. 1953. Propagation of radio waves over a stratified ground. Geophysics, v. 18 (2), p. 416-422. https://doi.org/10.1190/1.1437893

Windley, B.F., Allen, M.B. 1993. Mongolian Plateau: Evidence for a late Cenozoic mantle plume under central Asia. Geology, v. 21(4), p. 295-298. https://doi.org/10.1130/0091-7613(1993)021<0295:MPEFAL>2.3.CO;2

Zorin, Y.A., Novoselova, M.R., Turutanov, E.K., Kozhevnikov, V.M. 1990. Structure of the lithosphere of the Mongolian-Siberian mountainous province. Journal of Geodynamics, v. 11(4), p. 327-342. https://doi.org/10.1016/0264-3707(90)90015-M

APPENDIX A.
Magnetotelluric sounding curves of some MT sites

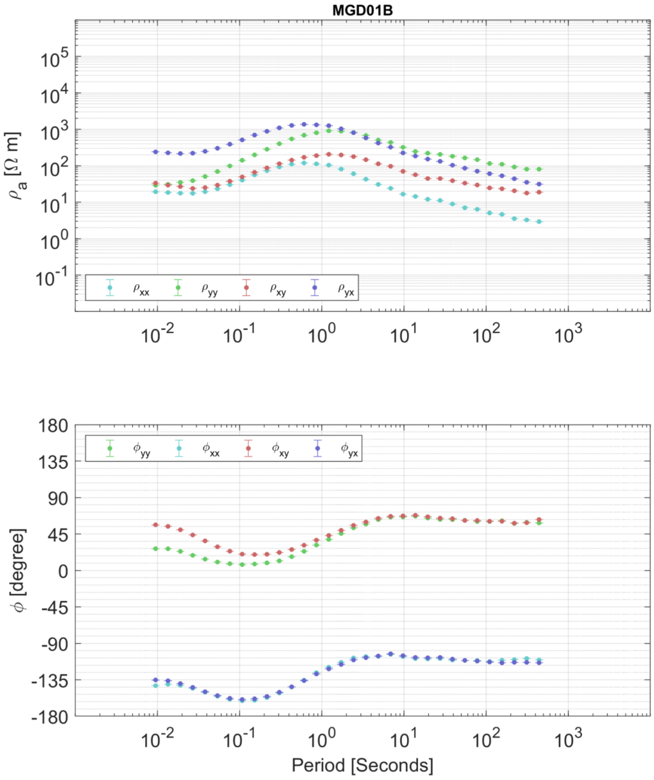

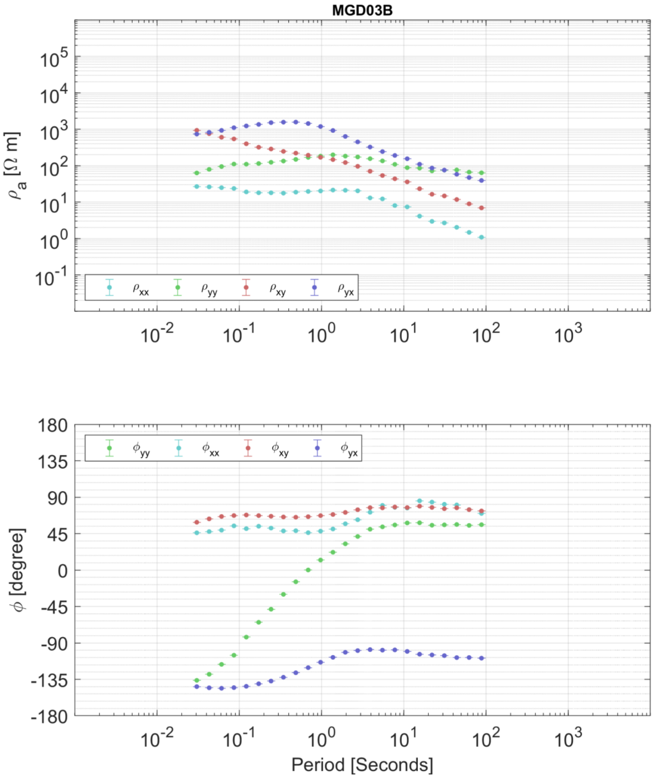

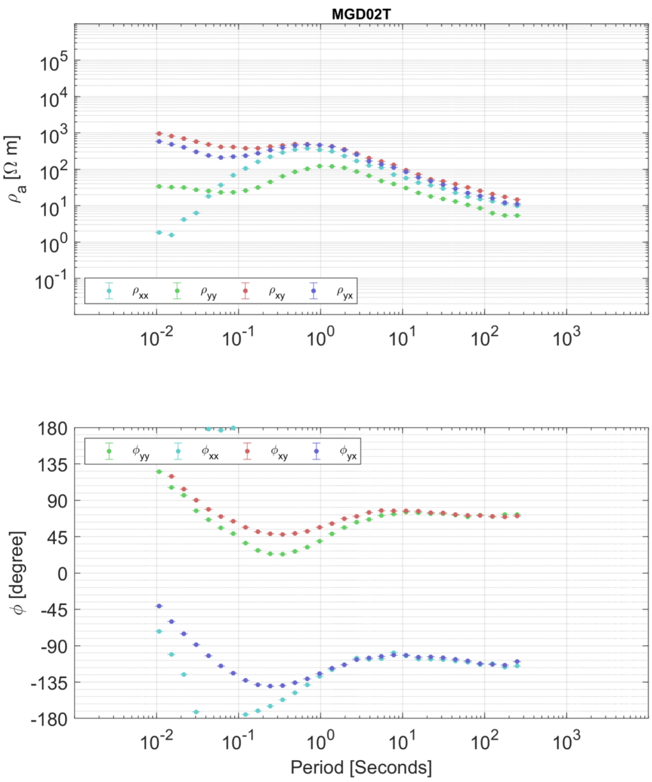

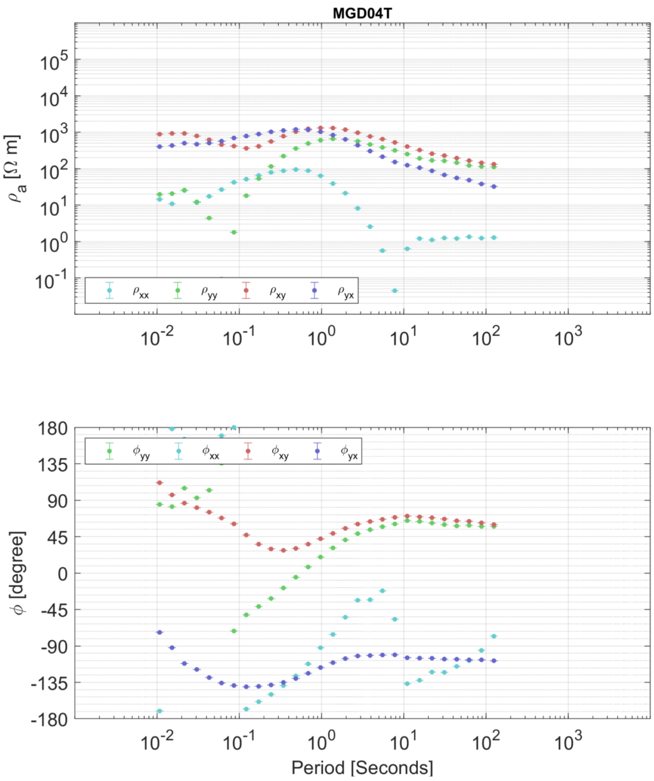

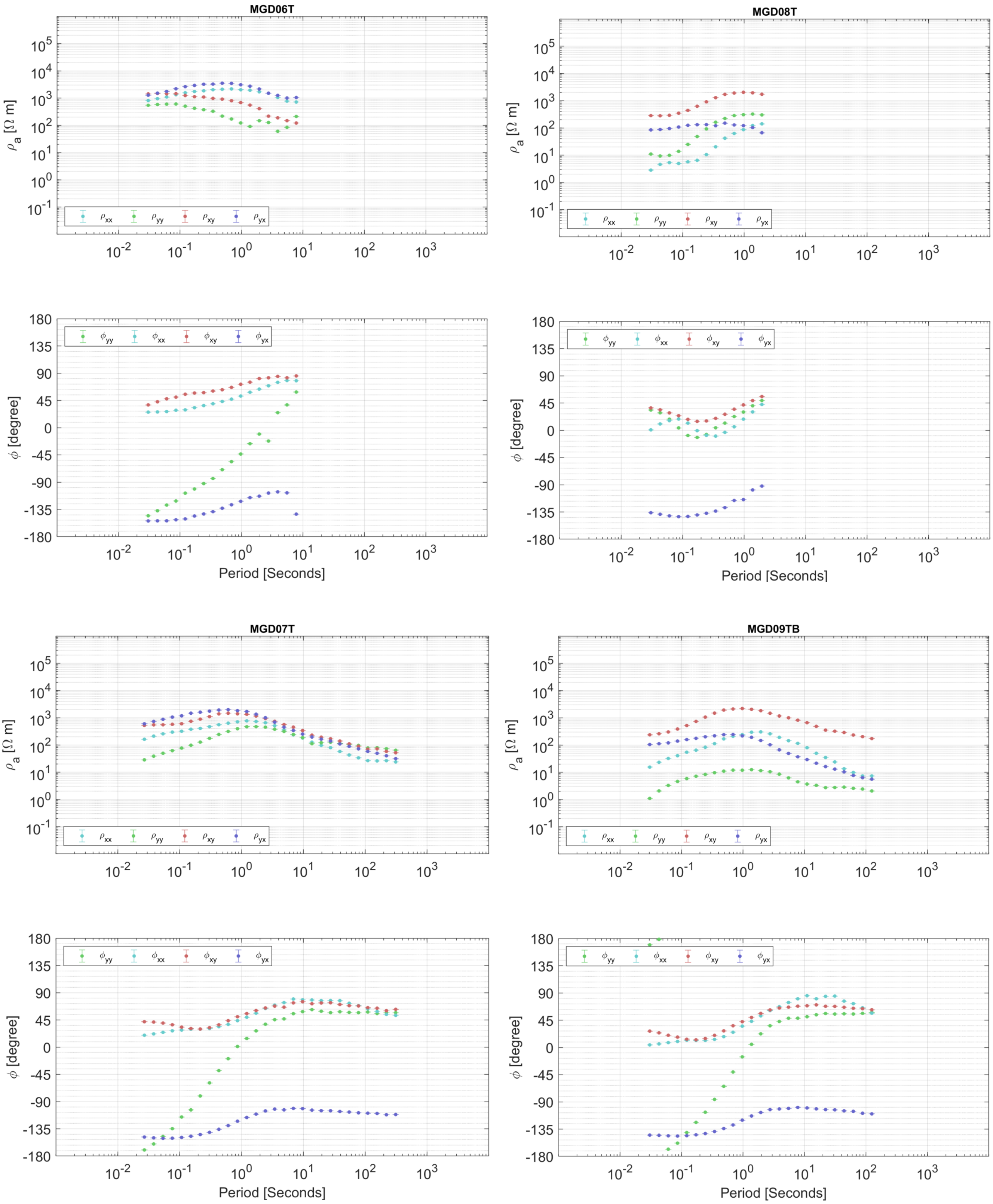
MGD06T
MGD08T
MGD07T
MGD09TB
ρa [Ω m]
φ [degree]
Period [Seconds]
ρxx ρyy ρxy ρyx
φyy φxx φxy φyx